

## **PREPARATION AND THERMAL DECOMPOSITION OF SOLID-STATE CINNAMATES OF LIGHTER TRIVALENT LANTHANIDES**

*M. A. S. Carvalho Filho*<sup>1</sup>, *N. S. Fernandes*<sup>1</sup>, *M. I. G. Leles*<sup>2</sup>, *R. Mendes*<sup>1</sup>  
and *M. Ionashiro*<sup>1\*</sup>

<sup>1</sup>Instituto de Química, UNESP, Araraquara, SP, C. P. 355, CEP. 14801-970

<sup>2</sup>Instituto de Química, UFG, Goiânia, GO, C. P. 131, CEP. 74002-970, Brazil

### **Abstract**

Some new compounds of cinnamic acid with lighter trivalent lanthanides were prepared in the solid state. The compounds have general formula  $ML_3 \cdot H_2O$ , where  $L$  is cinnamate ( $C_6H_5-CH=CH-COO^-$ ) and  $M$  is La, Ce, Pr, Nd or Sm. Thermogravimetry, derivative thermogravimetry, differential scanning calorimetry, infrared absorption spectra and X-ray diffraction powder patterns were used to characterize and to study the thermal stability and thermal decomposition of these compounds.

**Keywords:** cinnamate, lanthanides, thermal decomposition

### **Introduction**

Solid-state compounds of 4-dimethylaminobenzylidenepyruvate and 4-methoxybenzylidenepyruvate with a number of metal ions have previously been prepared and studied by complexometry, TG, DTG, DSC, DTA and X-ray powder diffractometry [1, 2]. Cinnamates of cobalt, nickel and copper have also been prepared and characterized via magnetic moment analysis, their vibrational and electronic spectra, and their thermal behaviour on TG and DTA [3].

This paper reports thermal analysis studies of lighter trivalent lanthanide cinnamates by means of TG, DTG and DSC.

### **Experimental**

The cinnamates of La, Ce, Pr, Nd and Sm were prepared by addition of an aqueous solution of the respective lanthanide nitrate to an aqueous solution of sodium cinnamate. The precipitates obtained were washed with distilled water and ethanol until elimination of nitrate ions and excess cinnamic acid, dried in a forced circulation oven at 50°C and kept in a desiccator over anhydrous calcium chloride.

\* Author to whom all correspondence should be addressed.

These compounds were studied by TG, DTG, DSC, IR absorption spectroscopy and X-ray diffractometry.

The metal contents of the compounds were determined by complexometric titration with standard EDTA solution, after samples of the compounds had been ignited to the metal oxide and dissolved in nitric acid solution. The water and cinnamate contents were determined from the TG curves.

The TG and DTG curves were recorded on a Perkin Elmer TGS-2 thermogravimetric system: samples of about 7 mg were used in platinum crucibles, heated at a rate of  $20^{\circ}\text{C min}^{-1}$  in air flowing at a rate of  $20 \text{ mL min}^{-1}$  at ambient pressure.

The DSC curves were obtained by using a Mettler TA-4000 thermal analysis system with air flowing at a rate of about  $150 \text{ mL min}^{-1}$ , a heating rate of  $20^{\circ}\text{C min}^{-1}$  and aluminum crucibles with perforated covers.

The X-ray powder patterns were obtained with an HGZ 4/B horizontal diffractometer (GDR) equipped with a proportional counter and a pulse height discriminator. The Bragg-Brentano arrangement was adopted, using  $\text{CoK}_{\alpha}$  ( $\lambda=1.7889 \text{ \AA}$ ) and a setting of 38 kV and 20 mA.

The IR spectra were recorded on a Nicolet FTIR-730 spectrophotometer in the spectral range  $4000\text{--}400 \text{ cm}^{-1}$ , using KBr pellets.

## Results and discussion

Table 1 presents the analytical and thermoanalytical (TG) data on the prepared compounds. The complexometric and TG results permitted determination of the hydration degree and establishment of the stoichiometry of the prepared compounds. In each case, the results indicated the relation  $M:L:H_2O=1:3:1$ . The TG curves also suggested that the water is strongly bound.

**Table 1** Analytical and thermoanalytical results

Compound	Ligand loss/%		Metal content/%		
	TG	calcd.	TG	calcd.	EDTA
$[\text{LaL}_3\text{H}_2\text{O}]_n$	69.5	69.78	23.2	23.21	23.85
$[\text{CeL}_3\text{H}_2\text{O}]_n$	68.7	68.30	23.3	23.37	23.15
$[\text{PrL}_3\text{H}_2\text{O}]_n$	68.8	68.65	23.5	23.47	23.24
$[\text{NdL}_3\text{H}_2\text{O}]_n$	69.0	69.15	23.8	23.89	23.47
$[\text{SmL}_3\text{H}_2\text{O}]_n$	68.7	68.46	24.7	24.65	24.45

*L*– cinnamate

The X-ray powder patterns verified that the compounds have a crystalline structure, with evidence of the formation of an isomorphous series.

Cinnamic acid has two different potential donor sites for the formation of bonds with metal ions: the carbon-carbon double bond and the carboxylic acid oxygen at-

oms. The IR spectra data were used to elucidate the coordination between the metals and the ligand.

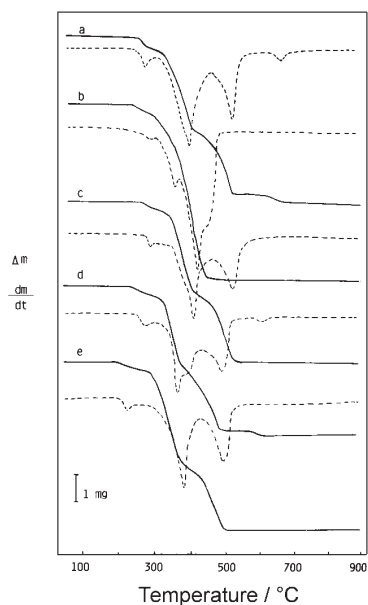
**Table 2** IR spectra ( $\text{cm}^{-1}$ ) of the complexes  $[\text{LnL}_3\text{H}_2\text{O}]_n$ , where  $\text{Ln}$  represents the lanthanides and  $L$  is cinnamate

Compound	$\nu_{\text{O-H}}(\text{H}_2\text{O})$	$\nu_{\text{COO}^-}$	$\nu_{\text{C=C}}$
LH	–	1679 (s)	1625 (s)
$\text{NaL}\cdot\text{H}_2\text{O}$	3100–3600	1549 (s)	1641 (s)
$[\text{LaL}_3\text{H}_2\text{O}]_n$	3060–3700	1502 (s)	1635 (s)
$[\text{CeL}_3\text{H}_2\text{O}]_n$	3053–3650	1500 (s)	1635 (s)
$[\text{PrL}_3\text{H}_2\text{O}]_n$	3052–3720	1499 (s)	1635 (s)
$[\text{NdL}_3\text{H}_2\text{O}]_n$	3112–3700	1503 (s)	1636 (s)
$[\text{SmL}_3\text{H}_2\text{O}]_n$	3055–3780	1502 (s)	1636 (s)

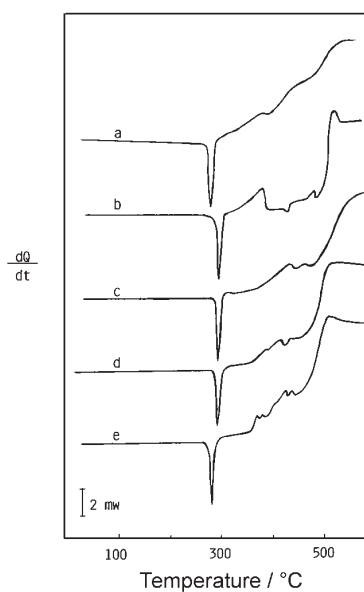
(s) – strong

Table 2 lists the main bands observed in the IR spectra. The bands in the region  $3700\text{--}3000\text{ cm}^{-1}$  are assigned to the  $\nu(\text{O-H})$  of water [4]. The bands in the region  $1635\text{--}1636\text{ cm}^{-1}$  are assigned to the  $\nu(\text{C=C})$  vibrations. It is suggested that coordination does not take place between the  $\pi$ -electron system of the  $\text{C=C}$  bond and the metal ions, because a change to lower frequency is not observed in the compounds. However, a significant change to lower frequency can be observed in  $\nu(\text{COO}^-)$  as compared with that for sodium cinnamate. This confirms that the coordination of the ligand to the metal ions proceeds via the  $\text{COO}^-$  groups. The electronic spectra and the magnetic moments for the cobalt and nickel compounds have been studied [5, 6]. The insolubility of the lighter lanthanide cinnamates in polar and non-polar solvents is in agreement with the literature data that suggest a polymeric structure [3, 4]. The TG and DTG curves of the compounds are shown in Fig. 1. These curves exhibit mass losses in two, three or four steps between  $200$  and  $680^\circ\text{C}$ , with the anhydrous cerium compound undergoing thermal decomposition in one step and with a lower final temperature of thermal decomposition, as can be seen from the TG/DTG curves in Fig. 1. The lower final temperature as compared with the other compounds is undoubtedly related to the exothermic oxidation reaction that results in the formation of cerium(IV) oxide.

These curves also demonstrate formation of the dioxycarbonate  $\text{Ln}_2\text{O}_2\text{CO}_3$  as intermediate only for the lanthanum and neodymium compounds. Tests with hydrochloric acid solution on samples heated up to the temperature of formation of the intermediate (as indicated by the TG/DTG curves) confirmed the elimination of  $\text{CO}_2$  and, in agreement with the calculations based on the TG data, suggested the formation of this intermediate.



**Fig. 1** TG and DTG curves of the complexes: a –  $[\text{LaL}_3\cdot\text{H}_2\text{O}]_n$  (6.98 mg); b –  $[\text{CeL}_3\cdot\text{H}_2\text{O}]_n$  (7.51 mg); c –  $[\text{PrL}_3\cdot\text{H}_2\text{O}]_n$  (6.97 mg); d –  $[\text{NdL}_3\cdot\text{H}_2\text{O}]_n$  (6.40 mg) and e –  $[\text{SmL}_3\cdot\text{H}_2\text{O}]_n$  (7.40 mg); L – cinnamate



**Fig. 2** DSC curves of the complexes: a –  $[\text{LaL}_3\cdot\text{H}_2\text{O}]_n$  (5.98 mg); b –  $[\text{CeL}_3\cdot\text{H}_2\text{O}]_n$  (6.42 mg); c –  $[\text{PrL}_3\cdot\text{H}_2\text{O}]_n$  (6.05 mg); d –  $[\text{NdL}_3\cdot\text{H}_2\text{O}]_n$  (5.98 mg) and e –  $[\text{SmL}_3\cdot\text{H}_2\text{O}]_n$  (5.97 mg); L – cinnamate

**Table 3** Simultaneous fusion and dehydration of the complexes  $[\text{LnL}_3\text{H}_2\text{O}]_n$ , where  $\text{Ln}$  represents lanthanides and  $L$  is cinnamate

Compound	Temperature/ $^{\circ}\text{C}$	$\Delta H/\text{kJ mol}^{-1}$	
$[\text{LaL}_3\text{H}_2\text{O}]_n$	298.7	217.2	endo
$[\text{CeL}_3\text{H}_2\text{O}]_n$	298.4	127.6	endo
$[\text{PrL}_3\text{H}_2\text{O}]_n$	298.7	110.8	endo
$[\text{NdL}_3\text{H}_2\text{O}]_n$	299.0	99.71	endo
$[\text{SmL}_3\text{H}_2\text{O}]_n$	284.8	127.9	endo

In all the TG curves, the first mass loss is due to dehydration, with the loss of  $1\text{H}_2\text{O}$ , and the last step is due to the final thermal decomposition, with formation of the respective oxide,  $\text{Ln}_2\text{O}_3$ ,  $\text{CeO}_2$  or  $\text{Pr}_6\text{O}_{11}$ .

The temperature range and the percentage mass loss observed in each step of the thermal decomposition are shown in Table 4.

**Table 4** Temperature range and the percentage mass loss observed in each step of the TG curves of the complexes  $[\text{LnL}_3\text{H}_2\text{O}]_n$ , where  $\text{Ln}$  represents lanthanides and  $L$  is cinnamate

Compound		Steps			
		first	second	third	fourth
$[\text{LaL}_3\text{H}_2\text{O}]_n$	$\theta/^{\circ}\text{C}$	250–320	320–410	410–520	600–680
	Loss %	2.9	38.7	27.2	3.6
$[\text{CeL}_3\text{H}_2\text{O}]_n$	$\theta/^{\circ}\text{C}$	230–290	290–460	–	–
	Loss %	2.7	68.7	–	–
$[\text{PrL}_3\text{H}_2\text{O}]_n$	$\theta/^{\circ}\text{C}$	260–310	310–410	410–530	–
	Loss %	2.9	38.7	30.1	–
$[\text{NdL}_3\text{H}_2\text{O}]_n$	$\theta/^{\circ}\text{C}$	220–300	300–380	380–490	550–620
	Loss %	3.1	38.3	27.3	3.4
$[\text{SmL}_3\text{H}_2\text{O}]_n$	$\theta/^{\circ}\text{C}$	200–260	260–380	380–520	–
	Loss %	2.7	38.0	30.7	–

The DSC curves of the compounds are depicted in Fig. 2. In all the curves, the endothermic peak at about  $300^{\circ}\text{C}$  is attributed to simultaneous fusion and dehydration. The evidence that the dehydration is associated with the fusion was provided by experiments on samples heated in a long glass test-tube under approximately the same conditions as those for the DSC curves. In these experiments, simultaneous fusion and water condensation were observed. Table 3 lists the enthalpies of fusion associated with dehydration. The exotherms in the range  $320\text{--}600^{\circ}\text{C}$  are attributed to the thermal decomposition of the anhydrous compounds, where the oxidation of the

organic matter takes place in consecutive steps, in correspondence with the mass losses observed in the TG curves.

Decomposition of the anhydrous compounds occurs immediately after the dehydration process, and the residual mass are in good agreement with the values required for the metal oxides.

## Conclusions

The TG curves and complexometry revealed a general formula for these complexes in the solid state.

The TG, DTG and DSC curves provided previously unreported information concerning the thermal stability and thermal decomposition of these complexes.

\* \* \*

The authors are grateful to FAPESP (Proc. 85/0853-1) and CNPq for financial support and to Rosemary Camargo Gabarron for aid in the preparation of the manuscript.

## References

- 1 L. C. S. Oliveira, C. B. Melios, M. S. Crespi, C. A. Ribeiro and M. Ionashiro, *Thermochim. Acta*, 219 (1993) 215.
- 2 D. E. Rasesa, L. C. S. Oliveira, C. B. Melios and M. Ionashiro, *Thermochim. Acta*, 250 (1993) 151.
- 3 J. R. Allan and B. R. Carson, *Thermochim. Acta*, 154 (1989) 315.
- 4 J. R. Allan, N. D. Baird and L. Kassyk, *J. Thermal Anal.*, 16 (1979) 79.
- 5 R. C. Stoufer, D. W. Smith, E. A. Clevenger and T. E. Norris, *Inorg. Chem.*, 5 (1966) 167.
- 6 L. S. Forster and C. J. Balhausen, *Acta Chem. Scand.*, 16 (1962) 1385.